

# The HIV-1 *rev* trans-activator acts through a structured target sequence to activate nuclear export of unspliced viral mRNA

Michael H. Malim\*, Joachim Hauber\*‡, Shu-Yun Le†, Jacob V. Maizel† & Bryan R. Cullen\*§

\* Howard Hughes Medical Institute and Department of Medicine, Duke University Medical Center, Durham, North Carolina 27710, USA

† Laboratory of Mathematical Biology, Division of Cancer Biology and Diagnosis, National Cancer Institute, National Institutes of Health, Frederick, Maryland 21701, USA

**HUMAN immunodeficiency virus type 1 (HIV-1) replication requires the expression of two classes of viral mRNA. The early class of HIV-1 transcripts is fully spliced and encodes viral regulatory gene products. The functional expression of one of these nuclear regulatory proteins, termed Rev (formerly Art or Trs), induces the cytoplasmic expression of the incompletely spliced, late class of HIV-1 mRNAs that encode the viral structural proteins, including Gag and Env<sup>1-6</sup>. Here, we provide evidence that this induction reflects the export from the cell nucleus to the cytoplasm of a pool of unspliced viral RNA constitutively expressed in the nucleus. The hypothesis that Rev acts on RNA transport, rather than splicing, is further supported by the observation that the cytoplasmic expression of a non-spliceable HIV-1 *env* gene sequence is also subject to Rev regulation. Here we show that this Rev response requires a specific target sequence which coincides with a complex RNA secondary structure present in the *env* gene. The response to Rev is fully maintained when this sequence is relocated to other exonic or intronic locations within *env* but is ablated by inversion. These results indicate that the HIV-1 *rev* gene product induces HIV-1 structural gene expression by activating the sequence-specific nuclear export of incompletely spliced HIV-1 RNA species.**

In the absence of Rev, the genomic HIV-1 *tat* gene expression vector pgTAT<sup>6</sup> (Fig. 1a) predominantly expresses a fully spliced cytoplasmic *tat* mRNA (Fig. 1b, lane 9) that encodes the 86-residue form of the HIV-1 Tat protein (Fig. 1c, lane 1). In the presence of Rev, pgTAT produces a high level of an unspliced cytoplasmic mRNA (Fig. 1b, lane 10), structurally equivalent to *env* mRNA<sup>6</sup>, that encodes a truncated, 72-residue Tat protein (Fig. 1c, lane 2). Because it has been proposed that Rev suppresses the splicing of HIV-1 transcripts<sup>1,7</sup>, we examined the effect of substituting heterologous splice donor (pInsSD) or splice acceptor and branch-point sequences (pInsSA) for the authentic pgTAT splice sites (Fig. 1a). In each case, these sequences were derived from the genomic rat preproinsulin II gene<sup>8</sup>, which is not itself responsive to Rev (see below). Nuclease S<sub>1</sub> protection analysis using probes which spanned the insulin gene splice donor (Fig. 1b, lanes 1-4) or splice acceptor (Fig. 1b, lanes 5-8) reveals that the transfected pInsSA and pInsSD vectors predominantly express spliced cytoplasmic mRNA in the absence of Rev. Although these chimaeric transcripts used the predicted insulin RNA splice sites (Fig. 1b, lanes 1, 3, 6, 7) co-expression of *rev* nevertheless induces a high level of unspliced cytoplasmic mRNA (Fig. 1b, lanes 4, 8). In the case of pInsSA, the induced expression of an unspliced cytoplasmic *tat* mRNA was confirmed by immunoprecipitation analysis (Fig. 1c, lanes 3, 4).

The retention of full Rev responsiveness by pInsSA and pInsSD showed that the *cis*-acting Rev response element (RRE) must lie within the intronic *env* sequences of pgTAT. A series of deletion (pΔ) mutants of pgTAT (Fig. 1a) revealed that

vectors retaining an intronic BglIII (B2) to HindIII (Hd) fragment also retained full Rev responsiveness (Table 1). All vectors lacking this sequence, however, exclusively express the 86-residue Tat encoded by the spliced *tat* mRNA, regardless of *rev* co-expression. To localize more precisely the RRE within the B2/Hd fragment, we reinserted a series of subfragments into pΔB2/Hd to generate the pi vectors (Fig. 1a). The responsiveness of these vectors to Rev (Table 1) showed that the RRE must be at least 104 and possibly more than 210 nucleotides (nt) in length (Fig. 1a). Reinsertion of the complete B2/Hd fragment in the inverted orientation (piH/A) fails to restore Rev responsiveness (Fig. 1b, lane 16).

To determine whether the function of the RRE depends on location, we reinserted the B2/Hd fragment at selected sites within the Rev non-responsive pΔB2/Hd vector (Fig. 1a). These relocation (pλ) vectors reveal that the RRE is fully functional both at other intronic sites (pλK and pλB1, Table 1) and when inserted at an exonic BamHI (Bm) site located 3' to the *tat* gene splice acceptor (pλBm) (Fig. 1c, lanes 9, 10). Insertion at an EcoRI (R) site located immediately 3' to the vector polyadenylation site (pλR) however, did not restore Rev responsiveness to pΔB2/Hd (Fig. 1c, lanes 11, 12). It seems therefore that the RRE can function at any location within the primary *tat* gene transcript when present in the sense orientation.

The minimal size of the RRE is relatively large, indicating that secondary structure, in addition to primary sequence, may be important for recognition of the RRE. Indeed, the sequence encoding the N terminus of the HIV-1 gp41 Env protein is consistent with a high level of secondary structure<sup>9</sup>, and in Fig. 2 we present a stable predicted RNA stem-loop structure, which fully encompasses the minimal RRE defined by mutational analysis. The extension of this 234-nt secondary structure beyond the minimal 210-nt RRE defined by piD/G and piB/G may explain the incomplete Rev responsiveness of these vectors (Table 1). Interestingly, the only other predicted structure of comparable significance within the HIV-1 genome coincides with the putative RNA target sequence for *trans*-activation by the viral *tat* gene product<sup>9-11</sup>.

Although the data indicate that the *rev* gene product regulates the cytoplasmic expression of unspliced HIV-1 mRNA by directly or indirectly interacting with an RNA secondary structure, the observation that the RRE can function at both exonic and intronic locations argues against a direct effect on viral

TABLE 1 Mutational definition of the HIV-1 Rev response element

Clone tested	Rev response	Clone tested	Rev response
pgTAT	+++	Reinsertions	
Substitutions		piA/H	+++
pInsSD	+++	piB/H	+++
pInsSA	+++	piB/G	++
Deletions		piB/E	—
pΔK/B1	+++	piC/F	—
pΔK/B2	+++	piD/G	++
pΔK/Hd	—	piA/D	—
pΔB1/B2	+++	piE/H	—
pΔB1/Hd	—	Inversions:	
pΔB2/Hd	—	piH/A	—
Relocations:			
pλK	+++		
pλB1	+++		
pλBm	+++		
pλR	—		

Different mutants of the parental pgTAT vector (Fig. 1a) were assayed for the Rev-induced expression of unspliced cytoplasmic *tat* mRNA by S<sub>1</sub> used elsewhere analysis (Fig. 1b) and immunoprecipitation (Fig. 1c). +++, full Rev response; ++, partial Rev response; —, no detectable Rev response. All constructions displayed the same phenotype as pgTAT in the absence of Rev coexpression.

‡ Present address: Sandoz Research Institute, A1235 Vienna, Austria.  
§ To whom correspondence should be addressed.

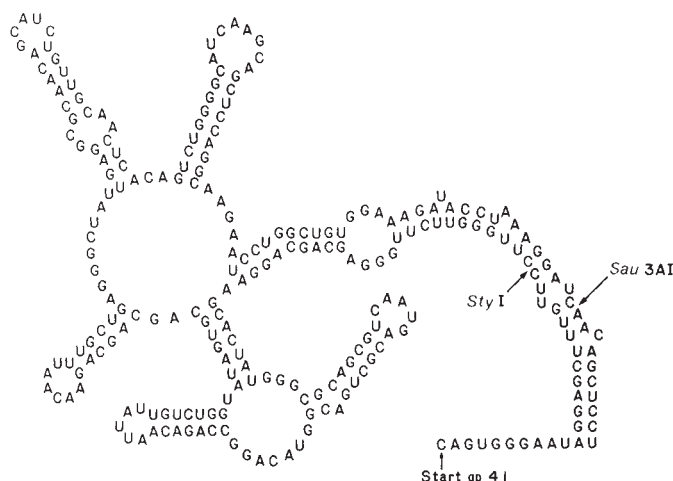
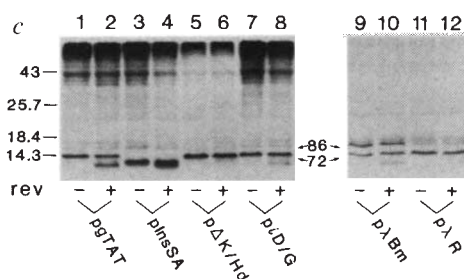
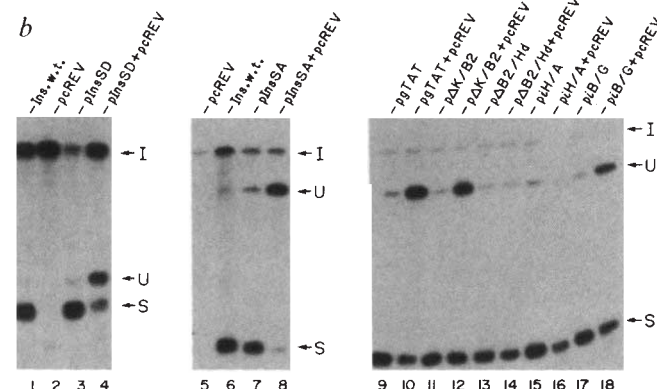


FIG. 1. Mapping of the HIV-1 Rev response element (RRE). *a*, The Rev responsive *tat* expression vector pgTAT contains the two HIV-1 *tat* gene-coding exons (hatched) separated by an *env*-gene-derived intronic element<sup>6</sup>. plnsSD and plnsSA were constructed by replacement of the authentic HIV-1 splice donor and splice acceptor elements with equivalent sequences from the genomic rat preproinsulin II gene expression vector pBC12M<sup>8</sup>. Deletion (pΔ) mutants were constructed by excision of sequences between intronic restriction-enzyme sites. The pAB2/Hd deletion mutant served as substrate for construction of the reinsertion (pi) and relocation (pλ) mutants. The names of the pi derivatives indicate which inclusive subfragment was reinserted. The pλ mutants were constructed by insertion of the complete A/H fragment at novel sites indicated by the vector name. The pENV160 vector lacks the HIV-1 SD sequence and instead proceeds from an *Avall* (V) site located immediately 5' to the *env* gene ATG<sup>3</sup>. pENV160 also contains 3' *env* gene sequences which overlap with, and extend 3' to, *rev* gene-coding sequences deleted from pgTAT. HIV-1 sequence coordinates (strain HXB-3) are relative to the start of the HIV-1 sequence at *Sall* at position 5,367 (ref. 18). S, *Sall*; 2, X, *Xho*II, 58; SD, splice donor, 260; V, *Avall*, 387; *env* initiation codon, 482; K, *Kpn*I, 564; B1, *Bgl*III, 1,254; B2, *Bgl*II, 1,834; M, *Mbo*II, 1,957; A1, *Alu*I, 1,986; St, *Sty*I, 1,994; Ha, *Hae*III, 2,058; D, *Dde*I, 2,103; A2, *Alu*I, 2,162; Sa, *Sau*3A1, 2,201; Hd, *Hind*III, 2,354; SA, Splice acceptor, 2,590; Bm, *Bam*HI, 2,688. Bs, *Bst*EII; W, *Alu*I; R, *Eco*RI. *b*, Quantitative S<sub>1</sub> nuclease protection analysis of cytoplasmic RNA isolated from COS cell cultures transfected with the indicated expression vectors<sup>6,8</sup>. Transfections were performed in the presence of the *rev* expression vector pcREV or the negative control vector pBC12/CMV<sup>6,8</sup>. The end-labelled, input probes (I) were designed to permit visualization of both unspliced (U) and spliced (S) cytoplasmic mRNA species. Ins. w.t., cultures transfected with the wild-type preproinsulin II gene expression vector pBC12MI (ref. 8). *c*, Immunoprecipitation analyses of transfected COS cell cultures were performed using anti-*tat* antisera<sup>6</sup>. Vectors were transfected in the presence (+) or absence (-) of the *rev* expression pcREV (ref. 6). The spliced pgTAT mRNA encodes an 86-residue protein whereas the unspliced mRNA encodes a 72-residue protein<sup>6</sup>. plnsSA lacks the second *tat* exon (Fig. 1*a*) and encodes a spliced mRNA predicted to give an 84-residue chimaeric *Tat* protein.

**METHODS.** *b*, The strategy for the  $S_1$  nuclease protection analyses has been described<sup>6</sup>. In each case, the DNA probe was end-labelled within a coding exon and extended into the flanking intron. A pBR322-derived tag permits the distinction of the input probe from the unspliced RNA signal. The probe used in Fig. 1*b*, lanes 1–4 was labelled at an insulin gene *Bam*HI (Bm) site using Klenow DNA polymerase I (Fig. 1*a*) and extends through the insulin gene splice donor (SD) at 174 nt (S) to an intronic *Eco*RI (R) site at 193 nt (U). The input probe was 386 nt in length. The probe used in Fig. 1*b*, lanes 5–8 was end-labelled at an insulin gene *A*/wI (W) site using polynucleotide kinase and extends through the insulin splice acceptor (SA) at 110 nt (S), to an intronic *Kpn*I (K) site at 378 nt (U). The input probe was 784 nt in length. The probe used in Fig. 1*b*, lanes 9–18 was end-labelled at a *tat* gene *Xho*II (X) site using Klenow DNA polymerase and extends through the *tat* gene splice donor (SD) at 202 nt (S) to an intronic *Kpn*I (K) site at 506 nt (U). The input probe was 798 nt in length.

FIG. 2 Predicted secondary structure of the HIV-1 Rev response element. The mutationally defined minimal RRE extends from a 5' StyI site to a 3' Sau3AI site (pID/G, Fig. 1a). This sequence is located immediately 3' to the start of the gp41 *env* gene-coding region and coincides with the most highly conserved sequence domain within the *env* gene<sup>9</sup>. The RNA stem-loop structure presented is both extremely stable ( $\Delta G = -115.1$  kcal/mol<sup>-1</sup>) and highly significant (segment score in standard deviation units = -5.29). In a previous survey, no equivalent predicted secondary structure was observed within the HIV-1 genome<sup>9</sup> and the RRE is therefore likely to be unique. In fact, the RRE would be contained within all known incompletely spliced HIV-1 mRNAs, including the *gag-pol* and *env* mRNAs.

**METHODS.** The distribution of significant secondary structures in the HIV-1 *env* gene was calculated for window (segment) sizes ranging from 30 to 300 bases by adding two bases to the segment size from 30 to 100 bases and five bases to the segment size from 100 to 300 bases. For each segment size, the calculation was carried out by sliding one base along the *env* gene-coding sequence. The segment scores which measure the statistical significance of the optimal secondary structures were computed<sup>9</sup> using the Cray operating system of a CRAY X-MP/24 computer and the energy rules of Salser<sup>19</sup> and Cech *et al.*<sup>20</sup>



RNA splicing. To examine the alternative hypothesis, that Rev activates the nuclear export of unspliced HIV-1 RNAs<sup>6</sup>, we used  $S_1$  nuclease analysis to quantify the effect of Rev on the level of spliced and unspliced *tat* RNA within the total, nuclear and cytoplasmic fractions of cells transfected with pgTAT. As an internal control, these cultures were cotransfected with a genomic rat preproinsulin II gene expression vector<sup>8</sup>. This experiment again showed that unspliced *tat* mRNA contributes only a low percentage of the cytoplasmic steady-state mRNA in the absence of Rev (Fig. 3a, lane 6) whereas unspliced cytoplasmic *tat* mRNA predominates in *rev*-expressing cells (Fig. 3a, lane 7). In contrast, unspliced *tat* RNA was the predominant *tat* RNA species detected in the nucleus regardless of *rev* co-expression (Fig. 3a, lanes 4, 5), indicating that Rev does not significantly affect either the nuclear stability or splicing of HIV-1 transcripts. Interestingly, the level of cytoplasmic unspliced *tat* mRNA expression induced by Rev closely mirrored the high level of unspliced RNA constitutively expressed in the nucleus. This is consistent with the hypothesis that Rev functions to equilibrate the cytoplasm with a pre-existing pool of nuclear viral RNA. The Rev protein also has little effect on the level of unspliced mRNA in total cellular RNA (Fig. 3a, lanes 2, 3), suggesting that the nuclear pool of HIV-1 RNA in these transfected cells contributes a surprisingly high percentage of total cellular HIV-1 RNA. A parallel analysis of insulin RNA expression (Fig. 3b) reveals that Rev had no detectable effect on the relative expression of spliced and unspliced insulin transcripts. By contrast with the simultaneously expressed *tat* RNA, unspliced insulin RNA was observed at only a very low steady-state level and was excluded from the cytoplasm. The high steady-state level of unspliced nuclear *tat* RNA in these transfected cells indicates that this HIV-1 RNA is poorly recognized by the nuclear splicing machinery. For other retroviruses, sequences have in fact been defined which act constitutively and in *cis* to reduce splicing efficiency<sup>12,13</sup>.

If the Rev protein acts to regulate the export from the nucleus to the cytoplasm of unspliced HIV-1 transcripts then it might also regulate the expression of genomic HIV-1 sequences which are incapable of splicing. In fact, Knight *et al.*<sup>3</sup> have previously shown that an *env* gene expression vector (pENV160, see Fig. 1a legend) which encodes a non-spliceable *env* RNA, remains fully subject to regulation by Rev<sup>3</sup>. Furthermore, the Rev induc-

tion of *env* protein is not accompanied by a significant increase in total cellular *env* RNA<sup>3</sup>. Our results (Fig. 3a) however, suggest, that the latter observation could have resulted from the use of unfractionated RNA in the earlier study. To clarify this, we transfected COS cells with pgTAT or with pENV160 in the presence or absence of Rev. Cytoplasmic RNA from these cultures was then subjected to northern analysis using an *env*-gene-specific probe. As previously reported<sup>6</sup>, unspliced cytoplasmic pgTAT RNA was observed only in the presence of Rev (Fig. 3c, lanes 3, 4). Remarkably, the cytoplasmic expression of the *env* mRNA encoded by pENV160 was also observed to be fully dependent on *rev* co-expression (Fig. 3c lanes 1, 2), showing that the regulation of cytoplasmic HIV-1 RNA expression by Rev occurs independently from the regulation of HIV-1 RNA splicing.

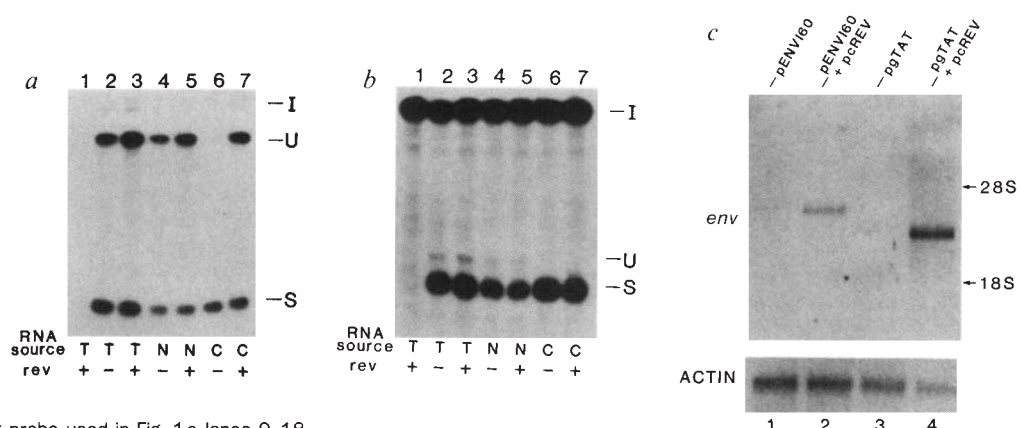
A major question raised by this study is why the high level of unspliced *tat* mRNA detected in the nucleus of transfected cells cannot enter the cytoplasmic compartment in the absence of Rev. One possibility is that the intronic sequences present in pgTAT repress unspliced RNA transport. Indeed, Rosen *et al.*<sup>14</sup> have proposed the existence of four such *cis*-acting repressive (CRS) sequences within the HIV-1 *env* gene. In the absence of *rev* co-expression, the deletion mutant pΔK/Hd, which lacks all four of these proposed repressive sequences, was, however, found to express the same phenotype as the parental pgTAT vector (Fig. 1c, lane 5). We therefore favour the alternative hypothesis that incompletely spliced HIV-1 mRNAs are prevented from leaving the nucleus by the same processes which preclude the export from the nucleus of many unspliced or incompletely spliced gene transcripts<sup>13,15-17</sup>. The role of Rev would then be to permit incompletely spliced HIV-1 transcripts to interact with the nuclear RNA export machinery. It remains to be determined if the Rev *trans*-activator mediates the export of unspliced viral RNA from the nucleus by interacting directly with its RNA target sequence or whether Rev instead functions to post-translationally or transcriptionally activate cellular RNA sequence-recognition factors. □

Received 20 January; accepted 2 February 1989.

1. Feinberg, M. B., Jarrett, R. F., Aldovini, A., Gallo, R. C. & Wong-Staal, F. *Cell* **46**, 807-817 (1986).
2. Sodroski, J. *et al. Nature* **321**, 412-517 (1986).
3. Knight, D. M., Flomerfelt, F. A. & Ghayab, J. *Science* **236**, 837-840 (1987).

FIG. 3 The *rev* gene product activates the nuclear export of unspliced HIV-1 RNAs. a,  $S_1$  nuclease analysis of spliced and unspliced *tat* gene RNA. COS cells were transfected<sup>6</sup> with pgTAT and the genomic rat preproinsulin II gene expression vector pBC12M in the presence (+) or absence (-) of the *rev* gene expression vector pcREV<sup>6</sup>. Lane 1 contains RNA from a culture transfected with pcREV alone. Total (T) or fractionated cytoplasmic (C) and nuclear (N) RNA was prepared at 48 h after transfection as previously described (21, 22). 5  $\mu$ g of RNA was used for the total and cytoplasmic  $S_1$  analyses while 2  $\mu$ g of RNA was used for the nuclear samples.

The input (I) probe is identical to the *tat* probe used in Fig. 1c, lanes 9-18 and allows the quantitation of both spliced (S) and unspliced (U) *tat* RNAs. The relative level of unspliced *tat* RNA in each sample was determined by densitometry using an LKB soft laser scanner and is: lane 2, 0.59; lane 3, 0.71; lane 4, 0.74; lane 5, 0.81; lane 6, 0.07; lane 7, 0.77. b,  $S_1$  nuclease analysis of spliced and unspliced insulin gene RNA. The analysis visualized here was performed precisely as described for Fig. 3a, using the same RNA samples, except that the insulin-gene-specific  $S_1$  probe described for Fig. 1c, lanes 1-4 was used. This input probe (I) permits the quantitation of both spliced (S) and unspliced (U) insulin RNA. c, Northern analysis<sup>23</sup> of cytoplasmic *env* gene mRNA. COS cell cultures were transfected<sup>6</sup> with pgTAT or pENV160 in the presence or absence of pcREV. As the *env* gene in pENV160 is under



HIV-1 LTR control, the *tat* gene expression vector pcTAT<sup>6</sup> was also included in each transfection. Cytoplasmic RNA was isolated<sup>21,22</sup> at 48 h after transfection and 5- $\mu$ g aliquots used for each lane. The unspliced RNA encoded by pgTAT is predicted to be 3.0 kilobases (kb) in length, whereas the non-spliceable *env* mRNA encoded by pENV160 has a predicted size of 3.5kb<sup>3,6</sup>. The filter was initially probed (upper panel) with an *env* gene specific probe derived from the *Bgl*II (B2) to *Hind*III (Hd) fragment shown in Fig. 1a. Subsequently, the filter was rehybridized with an actin probe as a loading control (lower panel).

4. Terwilliger, E. *et al.* *J. Virol.* **62**, 655–658 (1988).
5. Sadeie, M. R., Benter, T. & Wong-Staal, F. *Science* **239**, 910–914 (1988).
6. Malim, M. H., Hauber, J., Fenrick, R. & Cullen, B. R. *Nature* **335**, 181–183 (1988).
7. Gutman, D. & Goldenberg, C. J. *Science* **241**, 1492–1495 (1988).
8. Cullen, B. R. *Cell* **46**, 973–982 (1986).
9. Le, S.-Y., Chen, H.-H., Braun, M. J., Gonda, M. A. & Maizel, J. V. *Nucleic Acids Res.* **16**, 5153–5168 (1988).
10. Muesing, M. A., Smith, D. H. & Capon, D. J. *Cell* **48**, 691–701 (1987).
11. Feng, S. & Holland, E. C. *Nature* **334**, 165–167 (1988).
12. Katz, R. A., Kotler, M. & Skalka, A. M. *J. Virol.* **62**, 2686–2695 (1988).
13. Arrigo, S. & Beemon, K. *Molec. Cell Biol.* **8**, 4858–4867 (1988).
14. Rosen, C. A., Terwilliger, E., Dayton, A., Sodroski, J. G. & Haseltine, W. A. *Proc. natn. Acad. Sci. U.S.A.* **85**, 2071–2075 (1988).
15. Nevins, J. R. *A. Rev. Biochem.* **52**, 441–466 (1983).
16. Darnell, J. E. *Prog. Nucleic Acid Res. Molec. Biol.* **19**, 493–511 (1976).
17. Buchman, A. R. & Berg, P. *Molec. cell. Biol.* **8**, 4395–4405 (1988).
18. Ratner, L. *et al.* *Nature* **313**, 277–284 (1985).
19. Salsler, W. *Cold Spring Harb. Symp. quant. Biol.* **42**, 993–1004 (1977).
20. Cech, T. R. *et al.* *Proc. natn. Acad. Sci. U.S.A.* **80**, 3903–3907 (1983).
21. Greenberg, M. E. & Ziff, E. B. *Nature* **311**, 433–438 (1984).
22. Chirgwin, J. M., Przybyla, A. E., MacDonald, R. J. & Rutter, W. J. *Biochemistry* **18**, 5294–5304 (1979).
23. Thomas, P. S. *Proc. natn. Acad. Sci. U.S.A.* **77**, 5201–5205 (1980).

ACKNOWLEDGEMENTS. We thank John Ghayeb of Centocor for the pENV160 vector, Randy Fenrick and Sabine Bohnlein for technical assistance, and Sharon Goodwin for secretarial support.

## Signal transduction through the CD4 receptor involves the activation of the internal membrane tyrosine-protein kinase p56<sup>lck</sup>

André Veillette<sup>\*†</sup>, Michael A. Bookman<sup>†‡</sup>,  
Eva M. Horak<sup>†‡</sup>, Lawrence E. Samelson<sup>§</sup>  
& Joseph B. Bolen<sup>\*</sup>

Laboratory of Tumor Virus Biology<sup>\*</sup> and Medicine Branch<sup>†</sup>, National Cancer Institute and Cell Biology and Metabolism Branch, National Institute of Child Health and Human Development, National Institutes of Health<sup>§</sup>, Bethesda, Maryland 20892, USA

THE CD4 T-cell surface antigen is an integral membrane glycoprotein of relative molecular mass 55,000 which binds class II major histocompatibility complex (MHC) molecules expressed on antigen presenting cells (APCs). It is thought to stabilize physical interactions between T cells and APCs (for a review, see ref. 1). Evidence is accumulating that suggests that CD4 can transduce an independent signal during T-cell activation<sup>2–4</sup>. It has recently been shown that CD4 expressed on human<sup>5,6</sup> and murine<sup>6</sup> T cells is physically associated with the Src-related tyrosine protein kinase p56<sup>lck</sup> (refs 7, 8). These results indicate that CD4 can function as a signal transducer and suggest that tyrosine phosphorylation events may be important in CD4-mediated signalling. Here, we present evidence that cross-linking of the CD4 receptor induces a rapid increase in the tyrosine-specific protein kinase activity of p56<sup>lck</sup> and is associated with the rapid phosphorylation of one of the subunits ( $\zeta$ ) of the T-cell receptor complex on tyrosine residues. These data provide direct evidence for a specific CD4 signal transduction pathway that is mediated through p56<sup>lck</sup> and suggest that some of the tyrosine phosphorylation events detected during antigen-mediated T-cell activation may result from signalling through this surface molecule.

To test whether binding of ligand to the extracellular domain of CD4 results in an intracellular signal involving alterations of p56<sup>lck</sup>, we examined the effects of antibody-mediated cross-linking of cell-surface CD4 on the enzymatic activity of p56<sup>lck</sup> (Fig. 1). Cloned CD4<sup>+</sup>/CD8<sup>−</sup> murine T lymphocytes (C8, see Fig. 1 legend)<sup>9</sup> were incubated with anti-CD4 monoclonal anti-

body (mAb) GK1.5 (which reacts against the extracellular domain of CD4) and rabbit anti-rat (RAR) immunoglobulin G. The effects of this treatment on the tyrosine kinase activity of p56<sup>lck</sup> were analysed by immune-complex kinase assays using Lck-specific antisera (Fig. 1a). CD4 cross-linking resulted in a rapid (within 30 seconds) and significant (three to fivefold) increase in the tyrosine-specific protein kinase activity of p56<sup>lck</sup>, as measured by *in vitro* autophosphorylation and phosphorylation of enolase, an exogenous substrate. A parallel Lck immunoblot (Fig. 1a, bottom panel) showed that this change is not attributable to an increase in the abundance of p56<sup>lck</sup>, suggesting that it reflects an increase in 'specific' enzymatic activity. Similar results were obtained with another CD4<sup>+</sup> murine T-cell clone (B10; ref. 6) but were not observed in the CD4<sup>−</sup> murine T-cell hybridoma 16M9 (ref. 10). The abundance of the Lck protein seemed to diminish after a few minutes of cross-linking (bottom panel, lanes 4 and 5), consistent with our previous observations<sup>6</sup>.

The phosphorylated species migrating at about 64,000 (64K) on this gel appears to result from a non-specific immunoprecipitation (our unpublished data). Indeed, using lysis conditions that preserve the enzymatic activity of Lck as well as its interaction with CD4, another protein, p64, can be recovered by a variety of polyclonal and monoclonal antisera (including pre-immune sera). Although prominent in the C8 cells, it is not detected in murine thymocytes in which a similar stimulation of p56<sup>lck</sup> and enolase phosphorylation can be detected after CD4 cross-linking (manuscript in preparation). Preliminary data indicate that p64 may represent a contaminating serine kinase (unpublished data).

Further experiments (Fig. 1b) showed that the stimulation of Lck kinase activity depends on the physical cross-linking of CD4 as the enzymatic activity was unchanged by treatment with monovalent (antigen-binding) fragments (Fab) of mAb GK1.5 (Fig. 1b, lane 2). The small increase in kinase activity seen with mAb GK1.5 alone (lane 3) is probably a result of a small amount of CD4 cross-linking induced by the bivalent antibody or by aggregates of the monoclonal antibody. The specificity of the induction of Lck kinase activity by cell-surface antigen cross-linking was evaluated (Fig. 1c). Cross-linking of CD4 with a different anti-CD4 mAb (H129.19) (Fig. 1c, lane 3) also resulted in a rapid activation of p56<sup>lck</sup>. Cross-linking of other surface molecules however, such as the T-cell antigen receptor (TCR) complex, which can induce T-cell activation (lane 4), Thy1.2 (lane 5) as well as cross-linking antibody directed against CD8 (using an antibody with the same isotype as mAb GK1.5) (lane 6) did not result in any alteration in enzymatic activity or abundance of the Lck protein.

Because not all p56<sup>lck</sup> molecules expressed in CD4<sup>+</sup> T cells are complexed with CD4 (ref. 6), a more accurate estimate of the degree of enzymatic activation of p56<sup>lck</sup> requires a specific analysis of the population of Lck molecules associated with CD4. Immune-complex kinase assays of CD4 immunoprecipitates (Fig. 2a) revealed that CD4 cross-linking induced a six to eightfold increase in Lck kinase activity (Fig. 2a, lane 2). Additional experiments established that CD4 cross-linking did not significantly alter the enzymatic activity of the non-CD4 associated Lck kinase (Fig. 2b, lane 2).

The only substrate of an activated tyrosine kinase detected during antigen presentation that has been defined is the  $\zeta$ -subunit of the TCR complex, which is phosphorylated on tyrosine residues within minutes of antigen-mediated T-cell activation<sup>11–13</sup>. The data reported here raise the possibility that signalling through the CD4-Lck pathway may participate in this phosphorylation event. To determine whether CD4 cross-linking could mediate this alteration, the effect of antibody-mediated cross-linking of CD4 on the state of tyrosine phosphorylation of the  $\zeta$ -subunit of the TCR complex was examined (Fig. 3). After treating CD4<sup>+</sup> murine T cells (C8) in various ways, the components of the TCR complex were immunoprecipitated with

<sup>†</sup> Present addresses: McGill Cancer Center, McGill University, 3655 Drummond Street, Montreal, Canada H3G 1Y6 (A.V.); Fox Chase Cancer Center, Philadelphia, Pennsylvania, USA (M.A.B.); Laboratory of Tumor Virus Biology, National Cancer Institute, Bethesda, Maryland, USA (E.M.H.).